

# EMISSION OF COLLIMATED X-RAY RADIATION IN LASER-WAKEFIELD EXPERIMENTS USING PARTICLE TRACKING IN PIC SIMULATIONS \*

J. L. Martins<sup>†</sup>, S. F. Martins, R. A. Fonseca, L. O. Silva,  
GoLP/Instituto de Plasmas e Fusão Nuclear, Instituto Superior Técnico, Lisbon, Portugal  
C. Joshi, W. B. Mori, University of California Los Angeles, USA

## Abstract

It is now accepted that self-trapped electrons in a laser wakefield accelerator operating in the “bubble” regime undergo strong periodic oscillations about the wakefield axis because of the focusing force provided by the ions. This betatron motion of the off-axis electrons results in the emission of x-ray radiation strongly peaked in the forward direction. Even though the x-rays are broadband with a synchrotron-like spectrum, their brightness can be quite high because of their short pulse duration and strong collimation. We employ particle tracking in particle in cell simulations with OSIRIS, combined with a post-processing radiation diagnostic, to evaluate the features of the radiation mechanisms of accelerated electrons in LWFA experiments. We show and discuss results for a 1.5 GeV laser wakefield accelerator stage. A study of the angular dependence of the radiated power is also presented.

## INTRODUCTION

Particle in cell (PIC) codes have been successfully used for many years in plasma physics to address many different scenarios, such as collisionless shocks, laser-wakefield acceleration (LWFA) [1], fast-ignition, and many fundamental and applied plasma processes. However, in some conditions, the coexistence of spatial scales with different orders of magnitude raises challenging memory and computational requirements, since the algorithm resolves the smallest of these scales, usually on the electron time/space. Recently, the use of “boosted frames” has been suggested as a solution to this problem, in scenarios where it can reduce the gap between different spatial scales in the laboratory frame by running the simulation in a suitable relativistic moving frame [2, 3].

In problems where the focus is on the radiation being generated due to the motion of accelerated charged particles, other methods have been implemented to address the specific issue of determining the features of this radiation when its wavelength is much shorter than the other characteristic spatial scales of the simulation, namely the post-

processing of particle data (position and momentum over time) [4, 5]. These methods make use of the particle trajectory in phase-space, determined directly from the PIC simulations, to calculate the energy spectrum and radiated energy with well known electrodynamics formulas (see for eg. [6]). The goal is to obtain the spectral data beyond the resolution limit imposed by the numerical grid of the simulation. In this work we describe an implementation of a post-processing radiation diagnostic which takes advantage of the data mining features available in the OSIRIS framework [7, 8].

One of the scenarios where the post-processing diagnostic can give significant insight into the radiation being produced is in laser and plasma wakefield accelerators. Radiation originating from the electron motion inside the ion cavity due to the radial focusing force, the betatron radiation, is currently attracting great interest [4, 9, 10, 11, 12, 13, 14]. This is due to the short wavelength that can be achieved, which opens the possibility of reducing the cost and size of intense X-ray sources, by producing this high-energy radiation with a single LWFA, or with a LWFA coupled with an undulator [14]. In many laser wakefield scenarios the laser wavelength,  $\lambda_0$ , is on the order of hundreds of nanometers and the plasma density  $n_e = 10^{16} - 10^{19} \text{ cm}^{-3}$ , which gives a plasma wavelength of the order of  $\lambda_p \simeq 10 - 300 \mu\text{m}$ . If the betatron radiation in LWFA reaches the X-ray regime, the wavelength of the emitted radiation can reach the nanometer or Angstrom scale, orders of magnitude below the laser and plasma characteristic scales. In this context, only a dedicated diagnostic that uses high-resolution particle trajectories, which are not restricted to the numerical grid, can capture the information about the emitted radiation.

## POST-PROCESSING RADIATION DIAGNOSTIC

One of the main advantages of PIC algorithms is the possibility to access the full information about the particle dynamics, namely the position and the momentum as a function of time. If this information can be retrieved and stored for a selected number of particles, it is then possible to post-process the radiation associated with a particular track of a particle.

Particle tracking in PIC codes usually involves two steps [8]. In the first step, the simulation is performed and the information for all the particles at a given time step is stored (some selection process can already be in place at

\* Work partially supported by Fundação Calouste Gulbenkian, by Fundação para a Ciência e Tecnologia under grants SFRH/BD/35749/2007, SFRH/BD/39523/2007 and PTDC/FIS/66823/2006 (Portugal), and by the European Community - New and Emerging Science and Technology Activity, FP6 program (project EuroLeap, contract #028514). The simulations presented were produced using the IST Cluster (IST/Portugal), the Dawson cluster (UCLA), and the NERSC supercomputers.

<sup>†</sup> jlmartins@ist.utl.pt

this point). With this information, data mining of the relevant particles to be tracked can be performed, for instance, by selecting particles in a given region of (phase) space.

The information of the particles to be followed can then be saved, and is then used as input for a second simulation, identical to the first, where the tracks for the selected particles are going to be saved. This technique imposes significant challenges in terms of the ability to efficiently store the particle information in a massively parallel simulation.

The radiation diagnostic then uses the information from the particle trajectories, position and momentum over time, to determine the energy being radiated by an accelerated charged particle. Figure 1 shows an example of such trajectories, taken from a simulation of a 1.5 GeV LWFA stage.

A radiation diagnostic should cover two main features: (i) a spatially resolved diagnostic of the energy deposited in a “virtual detector”, and (ii) the spatially resolved energy spectrum in the “virtual detector”. Having these two main features implemented, a spatially and temporally resolved diagnostic follows in a straightforward way (even though the computational requirements of the diagnostic can become quite demanding).

The “virtual detector” mimics an experimental detector in order to facilitate comparisons with experiments, corresponding to a region of a plane, with a well defined position and dimensions, and with an associated resolution, both in space and in frequency (when applicable). Using this information, a grid of points in space and/or frequency is defined.

To determine the energy deposited in the detector plane, we employ the expression for the radiated power per unit of solid angle [6]:

$$\frac{dP(t')}{d\Omega} = \frac{e^2}{4\pi c^2} \frac{|\vec{n} \times [(\vec{n} - \vec{\beta}) \times \vec{\beta}]|^2}{(1 - \vec{n} \cdot \vec{\beta})^5} \quad (1)$$

where  $\vec{n}$  is a unit vector directed from the particle position at the time of radiation emission,  $t'$ , to the observation point,  $\vec{\beta}$  is the velocity of the particle (normalized to  $c$ ), and  $\vec{\beta}$  is the acceleration, with all quantities measured at  $t'$ . The energy deposited on the detector is obtained by integrating Eq. (1) in time and in solid angle. In this case, and for each  $t'$ , it is possible to perform the solid angle integration approximately by calculating Eq. (1) at the center of the cell, and multiplying it by the solid angle associated with the cell. This yields the power radiated through the solid angle defined by the cell. To convert this quantity to the power radiated into the detector cell it is only necessary to divide it by  $R(t')^2$ , where  $R(t')$  is the distance from the particle at time  $t'$  to the cell. In order to obtain the total energy radiated in the interval  $\Delta t'$ , we multiply the power by  $\Delta t'$ , and the total energy in each cell of the virtual detector is then the sum of the contributions from all time steps and from all particles (i.e.  $E_{\text{cell}} = \sum_{\text{all particles}} \sum_{\text{time}} \Delta\Omega_{\text{cell}} \Delta t' \frac{dP(t')}{d\Omega}$ ). In choosing the detector cell resolution and position relative the trajectory one must take into account the fact that charged rel-

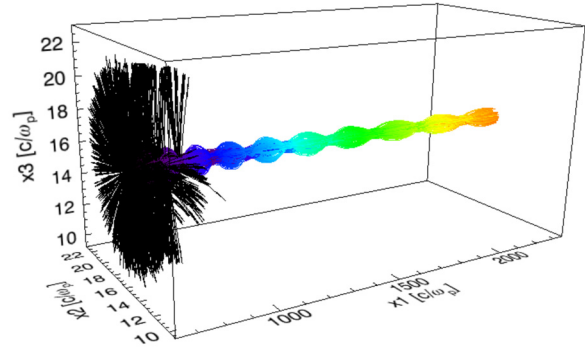


Figure 1: Sample of 1200 trajectories, represented in the laboratory frame, extracted from the electron bunch self-injected in the 1.5 GeV LWFA stage simulation. Color represents energy, from black to red, with the maximum energy being  $3400 m_e c^2 = 1.7$  GeV. The box size is  $7500 \times 60 \times 60 \mu\text{m}^3$ .

ativistic particles emit radiation with an angular aperture of the order of  $1/\gamma$ , where  $\gamma$  is the velocity relativistic factor.

The energy spectrum of the radiation emitted by an accelerated charged particle is given by [6]:

$$\frac{d^2 I(\omega)}{d\omega d\Omega} = \frac{e^2}{4\pi c} \left| \int_{-\infty}^{+\infty} \frac{\vec{n} \times [(\vec{n} - \vec{\beta}) \times \vec{\beta}]}{(1 - \vec{n} \cdot \vec{\beta})^2} e^{i\omega(t' + R(t')/c)} dt' \right|^2 \quad (2)$$

where  $\omega$  is the frequency of the radiation as seen by the observer. The energy spectrum is expressed as a function of angle. To calculate the energy spectrum at a given position of the virtual detector we replace the solid angle by  $dS/R(t')^2$  in the integration of Eq. (2). This integration is performed numerically, with the surface area element  $dS$  approximated by the area of the cell, thus yielding the radiated energy distribution.

## SIMULATION RESULTS

The post-processing diagnostic has been used to analyze the radiation emitted from self-injected electrons in a 1.5 GeV LWFA stage modeled in a three-dimensional simulation performed in a boosted frame (see [3]). The setup of our results corresponds to a LWFA stage where an 800 nm wavelength laser with a duration of 30 fs propagates through approximately 0.75 cm of plasma with a density of  $1.5 \times 10^{18} \text{ cm}^{-3}$ , in the laboratory frame. From the self-injected bunch observed in the simulation, with a total charge of 0.6 nC, a random sample of 5% of the self-injected electrons was taken and processed with our radiation diagnostic.

Figure 2 shows the energy radiated into an  $139 \times 139 \mu\text{m}^2$  detector placed  $\sim 2$  cm away from the end of the trajectories of the particles. The detector is centered with respect to the laser waist. The observed radiation pattern

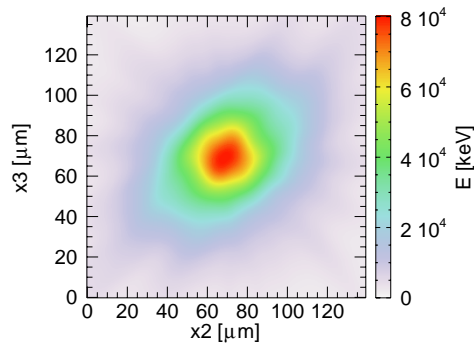


Figure 2: Energy radiated by the electron sample in the detector, in units of keV / pixel.

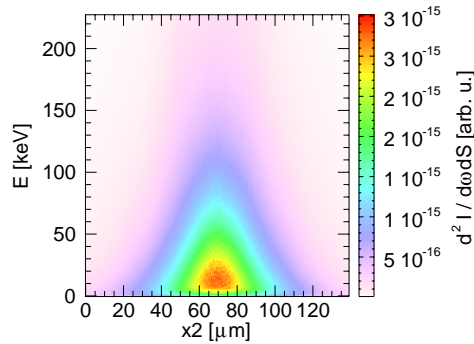


Figure 3: Spatially resolved energy spectrum for the sample of the bunch, in arbitrary units, determined in a horizontal lineout of the detector, vertically centered, with the horizontal axis representing the coordinates in  $x_2$  direction, and the vertical axis indicates the photon energy.

is consistent with the features of the betatron radiation for relativistic particles, a collimated beam of radiation in the direction of propagation with a FWHM angle divergence around  $\sim 2$  mrad. An estimate for the expected angular divergence can be obtained from the features of the trajectories. The typical radius of the betatron trajectory at the end of the simulations is  $r_\beta \simeq 1 \mu\text{m}$  for electrons with a Lorentz factor  $\gamma \simeq 3000$  which yields an angular divergence of the emitted radiation beam of  $a_\beta/\gamma \sim 3$  mrad, where  $a_\beta \simeq \gamma r_\beta \omega_p / c \sqrt{2\gamma}$  is the betatron strength parameter.

The spatially resolved spectrum shows that the energy of the radiated photon peaked on axis, as predicted by the theory, at energies close to 13 keV; this is due to the combination of the distribution of energies of the electrons within the bunch, the interval of radius of betatron motion, and the change in energy along the trajectories of the electrons due to the LWFA. The energy of the radiated photons extends up the full range of the diagnostic employed here (230 keV), with the energy spectrum in the 200 keV close to 10% of the peak of the energy spectrum at 13 keV.

## CONCLUSIONS

We have presented a massively parallel diagnostic that post-processes particle tracks to determine the energy radiated by the particles and the spectral features of this radiation. Using this tool, we have analyzed particle trajectories from a 1.5 GeV LWFA simulation, representing 5% of the self-injected electrons, and obtained photons in the 13 – 200 keV energy range with an angular divergence of 2 mrad. The main results agree with the theoretical predictions when all the features of the electron trajectories are taken into account.

## REFERENCES

- [1] Tajima, T. and Dawson, J.M., “Laser Electron Accelerator”, PRL, 43(4), 267 - 270 (1979).
- [2] Vay, J.L., “Noninvariance of Space- and Time-Scale Ranges under a Lorentz Transformation and the Implications for the Study of Relativistic Interactions”, PRL, 98(13), 130405 (2007).
- [3] Martins S. F. *et al.*, “Full-PIC 3D simulations of LWFA in boosted frames for long propagation distances”, AAC08 Proceedings 1086, 285-290 (2008).
- [4] Rousse, A. *et al.*, “Production of a keV X-Ray Beam from Synchrotron Radiation in Relativistic Laser-Plasma Interaction”, PRL, 93(13), 135005 (2004).
- [5] Hededal, C.B., “Gamma-Ray Bursts, Collisionless Shocks and Synthetic Spectra”, PhD thesis (2005); arXiv:astro-ph/0506559.
- [6] Jackson, J.D., “Classical Electrodynamics”, John Wiley & Sons, New York, ch. 14 (1998).
- [7] Fonseca, R.A. *et al.*, “Fully Relativistic Particle in Cell Code for Modeling Plasma Based Accelerators”, Lec. Notes Comp. Sci., 2331, 342-351 (2002).
- [8] Fonseca, R.A. *et al.*, “One-to-one direct modeling of experiments and astrophysical scenarios: pushing the envelope on kinetic plasma simulations”, PPCF, 50(12), 124034 (2008).
- [9] Wang, S. *et al.*, “X-ray Emission from Betatron Motion in a Plasma Wiggler”, PRL, 88(13), 135004 (2002).
- [10] Esarey, E. *et al.*, “Synchrotron radiation from electron beams in plasma-focusing channels”, PRE, 65(5), 056505 (2002).
- [11] Kostyukov, I., Kiselev, S. and Pukhov, A., “X-ray generation in an ion channel”, PoP, 10(12), 4818 (2003).
- [12] Kneip, S. *et al.*, “Observation of Synchrotron Radiation from Electrons Accelerated in a Petawatt-Laser-Generated Plasma Cavity”, PRL, 100(10), 105006 (2008).
- [13] Johnson, D. K. *et al.*, “Positron Production by X Rays Emitted by Betatron Motion in a Plasma Wiggler”, PRL, 97(17), 175003 (2006).
- [14] Schlenvoigt, H.-P. *et al.* “A compact synchrotron radiation source driven by a laser-plasma wakefield accelerator??”, Nat. Phys., 4, 130-133 (2008).
- [15] Gropp, W., Lusk, E., and Skjellum, A., “Using MPI”, MIT Press, 2<sup>nd</sup> ed., Cambridge (1999).